PTEN negatively regulates neural stem cell self-renewal by modulating G_0-G_1 cell cycle entry

Matthias Groszer*†‡, Rebecca Erickson*‡, Deirdre D. Scripture-Adams§¶, Joseph D. Dougherty‖, Janel Le Belle*, Jerome A. Zack§, Daniel H. Geschwind‖, Xin Liu*†, Harley I. Kornblum*‖**††, and Hong Wu*††

Departments of *Molecular and Medical Pharmacology, †Pathology and Laboratory Medicine, §Microbiology, Immunology, and Molecular Genetics, and **Pediatrics, and ‖Department of Neurology and The Neuropsychiatric Institute, David Geffen School of Medicine, University of California, Los Angeles, CA 90095

Communicated by Michael E. Phelps, University of California School of Medicine, Los Angeles, CA, November 16, 2005 (received for review October 3, 2005)

Previous studies have demonstrated that a small subpopulation of brain tumor cells share key characteristics with neural stem/progenitor cells in terms of phenotype and behavior. These findings suggest that brain tumors might contain "cancer stem cells" that are critical for tumor growth. However, the molecular pathways governing such stem cell-like behavior remain largely elusive. Our previous study suggests that the phosphatase and tensin homologue deleted on chromosome 10 (*PTEN*) tumor suppressor gene, one of the most frequently mutated genes in glioblastomas, restricts neural stem/progenitor cell proliferation *in vivo*. In the present study, we sought to determine the role of PTEN in long-term maintenance of stem cell-like properties, cell cycle entry and progression, and growth factor dependence and gene expression. Our results demonstrate an enhanced self-renewal capacity and G_0-G_1 cell cycle entry and decreased growth factor dependency of *Pten* null neural/stem progenitor cells. Therefore, loss of PTEN leads to cell physiological changes, which collectively are sufficient to increase the pool of self-renewing neural stem cells and promote their escape from the homeostatic mechanisms of proliferation control.

tumor suppressor | conditional knockout mouse model | growth factor dependency | brain tumor

The phosphatase and tensin homologue deleted on chromosome 10 (*PTEN*) tumor suppressor gene was the first phosphatase identified to be frequently mutated/deleted somatically in various human cancers, including glioblastoma multiforme (1–3). In addition, germline mutations in the *PTEN* gene have been associated with Cowden syndrome and related diseases in which patients develop macrocephaly of the brain and hyperplastic lesions in multiple organs with increased risks of malignant transformation (4, 5).

PTEN contains a sequence motif that is highly conserved in the members of the protein tyrosine phosphatase family. PTEN possesses phosphatase activity on phosphotyrosyl and phosphothreonyl-containing substrates (3, 6) *in vitro* and on phosphatidylinositol (3–5) trisphosphate, a product of phosphatidylinositol 3-kinase, both *in vitro* and *in vivo* (7–11). PTEN-deficiency leads to accumulation of PIP_3 and activation of signaling molecules that are critical in controlling cell size, cell migration, cell death, cell proliferation, and differentiation, all of which are involved in normal development and tumorigenesis (12).

We and other groups have used Cre-loxP technology to conditionally delete *Pten* in different regions of the brain and at different developmental stages (13–18). By crossing *Pten* conditional knockout mice with the Nestin-Cre line, we generated mutant mice with a substantially increased brain size and a doubled brain weight (13), similar to macrocephalic phenotypes found in humans with inherited PTEN mutations. Further studies indicated that the enlarged brain resulted from increased cell proliferation, decreased cell death, and enlarged cell size. Because all neural cell types are thought to be derived from a common stem cell, the neural stem cell, the overall size increase of the mutant brain prompted us to study the neural stem cell population. Our *in vitro* neurosphere culture analysis indicated that there were more stem cells in the mutant brain. Moreover, PTEN-deficient neural stem/progenitor cells have a greater proliferation capacity, which is due, at least in part, to a shortened cell cycle time (13).

One explanation for this phenomenon is that PTEN truly controls the stem cell self-renewing state and *Pten* deletion promotes neural stem cell self-renewal. In this case, we would expect to see a persistence of sphere-forming activity and maintenance of multilineage potential of *Pten* null neural stem cells in a long-term culture. Alternatively, effects of *Pten* deletion, seen both *in vivo* and *in vitro*, could have been due to enhanced proliferation of progenitors that were more limited in their differentiation potential. In this case, the number of *Pten* null spheres should remain the same, yet the size of the spheres should be greatly reduced. To distinguish between these two possibilities, in the current study, we performed stringent serial neurosphere passage experiments. Our results indicate that the loss of PTEN results in a prolonged self-renewal of neural stem/progenitor cells, without an appreciable change in their capacity for multipotential differentiation, whereas cortical stem/progenitor cells derived from WT animals had a limited capacity for self-renewal and gradually lost their capacity to produce neurons during the same culture period. Microarray analysis revealed prominent dysregulation of cell cycle-related genes in PTEN-deficient neurospheres. Furthermore, flow cytometric analysis indicated that PTEN-deficiency mediates enhanced neural stem/progenitor cell self-renewal by promoting exit from G_0/G_1A, and entrance into the cell cycle, in addition to the enhanced G_1-S transition reported in ref. 11. Taken together, these data suggest that the loss of PTEN confers an increased self-renewal capacity to neural stem/progenitor cells, a potentially important mechanism for brain tumorigenesis.

Results

PTEN Negatively Regulates Neural Stem Cell Self-Renewal *in Vitro*. To directly compare the properties of mutant (MUT) and WT stem/progenitors, we first examined the effect of PTEN deficiency on embryonic day (E) 14.5 cortices, an age when *Pten* deletion is just complete. Cells were subjected to serial stringent, low-density passaging (Fig. 1*A*), and their ability to form neurospheres was recorded after each passage. As shown in Fig. 1*B*, although spheres from ≈80% of the MUT animals were capable

Conflict of interest statement: No conflicts declared.

Abbreviations: E*n*, embryonic day *n*; MUT, mutant; PTEN, phosphatase and tensin homolog deleted on chromosome 10.

‡M.G. and R.E. contributed equally to this work.

¶Present address: Division of Biology, California Institute of Technology, Pasadena, CA 91125.

††To whom correspondence may be addressed. E-mail: hkornblum@mednet.ucla.edu or hwu@mednet.ucla.edu.

CELL BIOLOGY

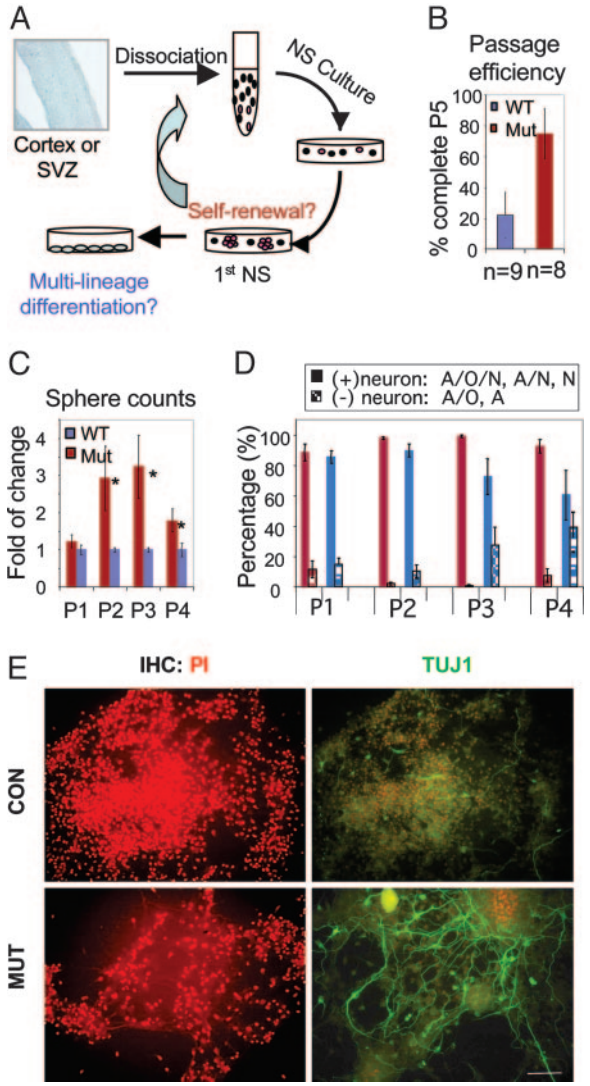

Fig. 1. PTEN loss leads to greater and persistent self-renewal capacity. (*A*) A schematic illustration of the serial neurosphere culture system. (*B*) Percentages of WT and MUT sphere cultures that can be serially passaged. (*C*) Sphere formation relative to WT sphere counts at each passage. (*D*) Histograms show the neurogenic potential of WT (in blue) and MUT (in red) neurosphere cultures. WT spheres demonstrated a loss of neurogenic potential over time with serial, low-density passages. Filled bars, spheres with neuron; hatched bars, spheres without neuron. (*E*) Representative images of the neurogenic potential of control and mutant neurospheres, with propridium iodide staining in *Left* and TuJ1 immunostaining in *Right*. (Scale bar: 17 μm.) A, GFAP$^+$ astrocytes; O, O4$^+$ oligodendrocytes; N, Tuj1$^+$ neurons.

of forming spheres for at least five passages (P5), only ≈20% of the WT cultures could do the same, owing to a lack of sufficient viable cells for reseeding.

To further explore the role of PTEN in neural stem/progenitor cell self-renewal, we quantified the number of spheres produced during each passage. *Pten* deletion resulted in a greater number of spheres, especially at passages 2, 3, and 4 (Fig. 1*C*). This result indicates that MUT cultures have a greater percentage of sphere-forming cells at each passage after initial plating, consistent with an increased self-renewal capacity. Because our neurosphere cultures were reseeded at a specific cell density, the results shown in Fig. 1*C* underestimate the total sphere-forming potential of MUT stem cells over time. To account for this underestimation, we estimated the total sphere-forming capacity (i.e., the number of spheres predicted if all cells from an individual culture were reseeded). These calculations demonstrate an exponential difference between MUT and WT sphere-forming capacity (Fig. 5, which is published as supporting information on the PNAS web site).

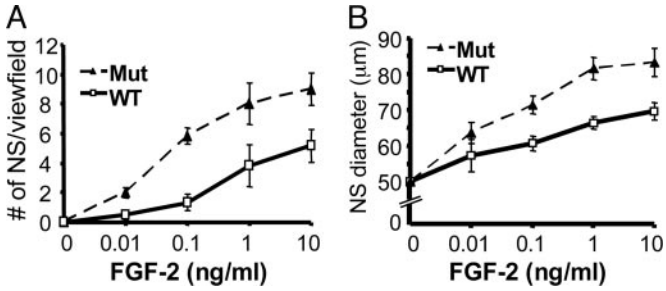

Fig. 2. *Pten* null neurospheres are hypersensitive to growth factor stimulation. Identical number of cells from WT and MUT E14.5 front brains were seeded in neurosphere cultures with the indicated concentration of FGF2. Neurosphere numbers (*A*) and size (*B*) were measured 7 days after initial culture and presented as mean ± SD.

***Pten* Null Spheres Are Multipotent and Have Greater Proliferation Capacity.** Neural stem cells can undergo multilineage differentiation and give rise to neurons, astrocytes, and oligodendrocytes (19). To verify that the effects observed above are indeed on neural stem cells, rather than committed progenitors, we evaluated the differentiation potential of WT and MUT spheres after each passage. As shown in Fig. 1 *D* and *E* (see also Fig. 6, which is published as supporting information on the PNAS web site), MUT spheres were multipotent and retained a similar capacity to produce neurons and glia throughout the experiment, suggesting that self-renewal was maintained. In contrast, WT spheres demonstrated a loss of neurogenic potential over time with serial, low-density passages (Fig. 1 *D* and *E*), consistent with the findings by others that cortically derived progenitors become more glial-restricted over time (20). These data indicate that PTEN loss not only supports persistent self-renewal, but maintains multilineage cell differentiation potential, resulting in a sustained neural stem cell-like state.

MUT spheres were significantly larger at all passages measured (Fig. 7, which is published as supporting information on the PNAS web site), similar to our previous study (13). As the passage number increased, the differences in sphere size became more significant (Fig. 7). In those few cases in which WT spheres could be passaged beyond four times, the differences in sphere size were quite striking (Fig. 7 *Left*). These data are consistent with the notion that PTEN loss enhances neural stem/progenitor proliferation over multiple passages, although concomitant effects on cell survival and cell size (see below) could account for some of the differences seen in neurosphere size.

Pten Null Neural Stem/Progenitor Cells Have Diminished Requirement for Growth Factor Stimulation. In the neurosphere culture system, neural stem cells undergo self-renewing cell divisions in basic medium supplemented with FGF2. To further understand PTEN controlled stem cell self-renewal, we conducted growth curve analyses by supplementing neurosphere cultures with different concentrations of FGF2. More neurospheres can be generated from MUT cortices than those of WT, even at suboptimal concentrations (Fig. 2*A*), indicating that MUT stem/progenitor cells are hypersensitive to FGF2 stimulation. Similarly, MUT spheres are larger, even in the presence of 100-fold less growth factor (0.1 ng/ml, Fig. 2*B*), although PTEN loss alone did not render neural stem/progenitor cell growth factor-independent. These results indicate that PTEN is a potent

negative regulator of the FGFR signaling pathway and neural stem cell self-renewal and proliferation. Furthermore, decreased reliance on growth-factor signals, a hallmark of cancer cell biology (21), might also be important for mobilizing stem cells from the quiescent stage (see below).

PTEN Negatively Regulates Entry into Cell Cycle. Somatic stem cells rapidly respond to stress, such as tissue damage, by generating progenitors and terminally differentiated cell types to replenish damaged areas. Concurrently, stem cells also generate additional stem cells, via amplification, before returning to quiescence. Although stem cell cell cycle entry and exit happen naturally *in vivo*, little is known about the genes and molecular mechanisms controlling this process.

Using a CFSE washout experiment, we previously demonstrated that PTEN deficiency leads to an increased number of cell divisions in neural stem cells (13). This observation prompted us to assess whether PTEN plays an important role in controlling exit from the G_0/G_1A (quiescent) stage of the cell cycle, and entry into the G_1B and $S/G_2/M$ stages of the cell cycle (see *Materials and Methods*). Using two-color flow cytometry, we labeled DNA and RNA simultaneously within fresh, dissociated brain (Fig. 3*A Upper*) and in cultured neurospheres (Fig. 3*A Lower*) (22).

A significant fraction of WT cells, either from the E14 forebrains or derived from dissociated first passage of neurosphere cultures, were in the quiescent G_0/G_1A cell cycle stage (Fig. 3*A Left*), consistent with previous studies (23). *Pten* null brains or neurosphere cultures, however, contained significantly fewer cells in the G_0/G_1A cell cycle stage, as compared to their age- and genetic background-matched littermates (Fig. 3*A Right*). Fig. 3*B Left* presents results from all experiments performed (*, statistically significant).

Our previous study suggests that PTEN negatively controls cell growth or size (13). To investigate whether cell size control is correlated with cell cycle regulation, especially exit from quiescence and cell cycle entry, we measured relative cell size at different cell cycle stages flow cytometrically by assessing forward scattered light. All cycling cells (G_1B, S, and G_2/M) from WT E14 forebrain or neurosphere cultures had higher forward scatter values than G_0/G_1A cells, indicating that the G_0/G_1A cells were smaller (Fig. 3*B Right*, in red). Similar to our previous report, cells from *Pten* null brain are, on average, bigger at every phase of cell cycle (Fig. 3*B Right*, in blue), although at the quiescent G_0/G_1A cell cycle stage, the mean forward scatter value measured for *Pten* null cells was not substantially different from that of the WT (Fig. 3*B*, *Right*). This result suggests that enhanced cell growth may push *Pten* null cells to enter the G_1B phase of the cell cycle, resulting in a decreased G_0/G_1A cell population. This finding is generally in agreement with the notion that cell growth or size control is largely regulated at the translational level (24).

PTEN Negatively Regulates Genes Involved in Cell Growth and Cell Cycle Control. The data described above support the hypothesis that loss of PTEN results in a greater self-renewal capacity of neural stem/progenitor cells. To further examine potential mechanisms of PTEN controlled neural stem/progenitor cell proliferation, we undertook an unbiased approach by analyzing the gene expression profiling of MUT and WT neurospheres.

We identified 257 genes that differ between MUT and WT neurosphere cultures at a confidence level of $P < 0.001$. We then performed hierarchical clustering (25) of differentially expressed genes. As expected, the six arrays clustered into two major groups according to the genotype (Fig. 4*A*). These differentially expressed genes can be further clustered into two major groups (marked by white boxes): genes that are up-regulated in the MUT (upper box) and genes that down-regulated in the MUT (lower box).

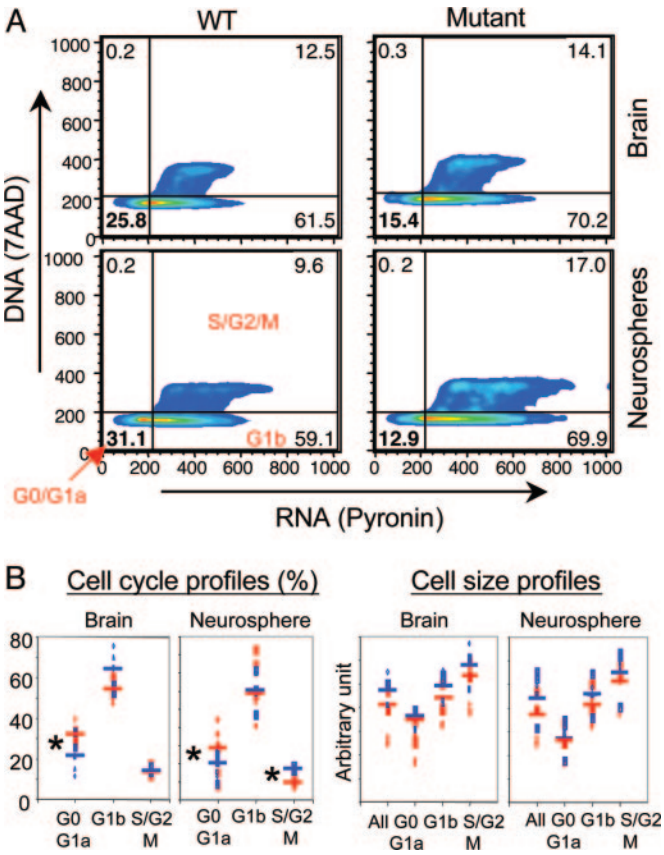

Fig. 3. Loss of PTEN leads to increased G_0/G_1A to G_1B cell cycle transition as well as increased cell growth. (*A*) Flowcytometric analysis of cell cycle status in primary cells from E14.5 cortices (*Upper*) and cells that have gone through one generation of neurosphere culture (*Lower*). *Left*, WT; *Right*, MUT. *N*-butyrate treated neurosphere cultures, which are arrested at the G_1A to G_1B transition, were used to demarcate the line (vertical axes) between cells falling into the G_0/G_1A stage (quiescence, *Lower Left*) and cells which have entered the G_1B stage of the cell cycle (*Lower Right*). (*B Left*) A comparison of cell cycle profiles. Statistic analysis for brain: G_0/G_1A, $P = 0.05$; G_1B, $P = 0.08$; $S/G_2/M$, $P = 0.43$; neurosphere: G_0/G_1A, $P = 0.05$; G_1B, $P = 0.72$; $S/G_2/M$, $P = 0.00003$. *, statistically significant. (*Right*) Cell size profiles at different cell cycle stages. Data include all experiments conducted. For brain, WT, $n = 10$; Mut, $n = 5$; for neurosphere, WT, $n = 11$; Mut, $n = 7$.

The most significantly up-regulated genes in the MUT spheres were cell cycle- and DNA replication-related genes, such as cyclin B1, cyclin B2, cyclin D1, cyclin E1, Ki-67, and DNA primases. Other examples of genes found to be up-regulated in MUT spheres include PBK/TOPK and maternal embryonic leucine zipper kinase, which have previously been identified by our group as being enriched in neural progenitors (26). Examples of genes found to be up-regulated in WT spheres were primarily related to cell differentiation and metabolism such as doublecortin, glutamate receptor (AMPA2), GABA receptor, and glutamate dehydrogenase.

To gain a more systematic understanding of the results of the gene expression analysis, we used the National Institutes of Health's DAVID software to classify our results into Gene Ontology categories (Fig. 4*B*, EASE $P < 0.5$). This analysis would help to identify biological processes that are significantly different between MUT and control cells. Results from Gene Ontology analysis identified a highly significant ($P < 2.7 \times 10^{-22}$, EASE statistic) overrepresentation of genes involved in regula-

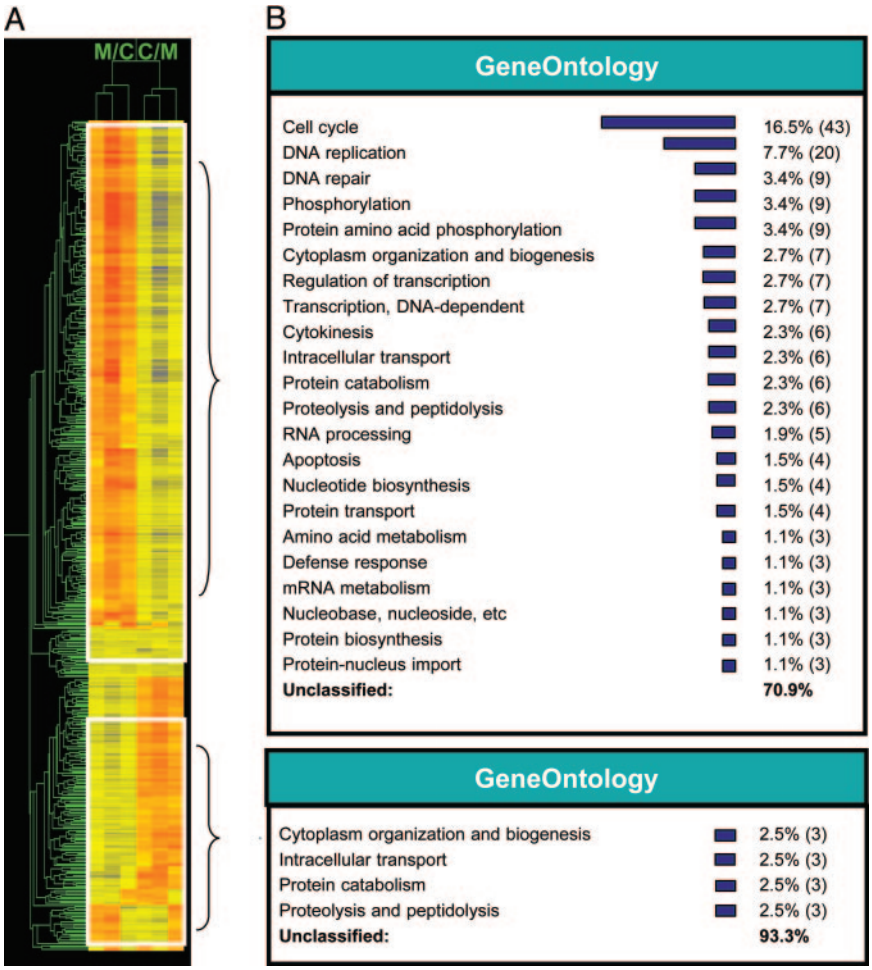

Fig. 4. Gene expression analysis. (*A*) Microarray data can be classified into two major groups, genes that are up-regulated in *Pten* null neurosphere cultures (upper box) and genes that are down-regulated in *Pten* null neurosphere cultures (lower box). (*B*) Gene Ontology analysis.

tion of the cell cycle as a key theme in the suite of gene expression of the knockout cultures, along with DNA replication, repair and cytokinesis. A complete list of those differentially regulated genes is shown in Tables 1 and 2, which are published as supporting information on the PNAS web site.

Discussion

To escape normal tissue homeostasis, tumor cells must acquire multiple genetic aberrations that collectively establish the malignant phenotype (21). For glioblastoma multiforme, this protracted process might encompass several years and requires brain tumor cells to maintain self-renewal capacities over extended periods. Previously, we and others have demonstrated that only a fraction of brain tumor cells have the ability to self-renew and to maintain brain tumor growth (27–29). Although these observations are now well documented, the molecular mechanisms governing these stem cell-like capabilities in brain tumors remain largely elusive (29). *PTEN* mutation is one of the most frequent genetic alterations associated with glioblastoma multiforme (30–32). Our previous study indicates that deletion of *Pten* in the embryonic brain leads to increased neural stem/progenitor cell proliferation (13). In the present study, we sought to determine whether loss of PTEN in neural/stem progenitor cells promotes the long-term maintenance of stem cell characteristics and the mechanisms underlying this maintenance.

Loss of PTEN in neural progenitors confers on them a greater capacity for persistent self-renewal. Although sphere forming activity in WT neurosphere cultures diminishes over time, consistent with previous studies (33), *Pten*$-/-$ neurosphere cultures can be stably maintained, suggesting that loss of PTEN is sufficient for the propagation of self-renewal properties. Consistent with this hypothesis, Sinor *et al.* (34) recently demonstrated that overexpression of Akt-1, a critical downstream target of PTEN signaling, results in enhanced self-renewal of cortical progenitor cells.

It is unknown at present whether deletion of PTEN would result in a similar phenotype in progenitors derived from other embryonic regions or from the subventricular zone derived from adult brain. Differences in the molecular mechanisms of self-renewal are clearly present in embryonic and fetal neural stem cells. For example, Bmi-1, a polycomb transcription factor, regulates neural stem cell self-renewal *in vivo* at postnatal, but not prenatal, stages, probably because fetal neural stem cells do not express the cell cycle inhibitory proteins that are regulated by Bmi-1 *in vivo* (35).

PTEN-deficient neurospheres retained their neurogenic potential, and we did not observe stem cell "exhaustion" in PTEN-deficient neurospheres derived from the embryonic cortex. These findings, taken together, indicate that a deletion of PTEN truly enhances stem cell self-renewal, rather than simply promoting the proliferation of committed progenitors or those with a limited capacity to self-renew. These findings are seemingly in contrast to those of Kippin *et al.* (36), who studied P21$-/-$ neurospheres derived from postnatal subventricular

zone. P21 is a regulator of the G_1 to S cell cycle progression. The neurospheres derived from adult animals rapidly exhausted their capacity to produce new neurospheres upon passaging. It is interesting to note, however, that neurospheres derived from younger P21-deficient animals had a more prolonged period of enhanced self-renewal than those derived from older animals.

In the adult, stem cells represent a relatively quiescent subpopulation, which can enter the cell cycle upon growth factor stimulation to replenish specific cellular populations and then exit the cycle to reside in their niche (G_0 cell cycle state) (37). However, given the importance of the G_0 cell cycle state for stem cell biology, little is known about the molecular mechanisms governing its establishment and maintenance. Results from a comprehensive screen of 6,000 gene deletion mutants in *Saccharomyces cerevisae* by Jorgensen *et al.* (38) revealed a close link between cell growth and cell cycle commitment. Their study suggests that, upon growth factor stimulation, cells grow to a critical size before entering the cell cycle and that the cell size increase, in turn, might be driven by an enhanced translational capacity. Importantly, one of the mutants identified is *sch9*, an ortholog of mammalian Akt, which also regulates longevity and stress resistance (39). Several studies in flies (40), yeast (41), and mammals (42) now suggest the existence of a similar link between cell growth and cell cycle commitment. Our observation, that cycling cells differ in cell size between WT and *Pten* null neural stem/progenitor cells but differ less in quiescent G_0 cells, is in agreement with above-mentioned studies and indicates that the PTEN-AKT-TOR pathway, by regulating protein synthesis and cell growth, may play an important role in cell cycle commitment.

The enhanced self-renewal capacity, cell cycle commitment, and proliferation potential of *Pten*-deficient neurospheres are reflected in their gene expression profile. The maternal embryonic leucine zipper kinase is enriched in embryonic and adult neural stem/progenitor cells and is required for their self-renewal capacity (43). Because maternal embryonic leucine zipper kinase is not a direct target of the PTEN signaling pathway (43), its up-regulation suggests an enrichment of cells with self-renewal capacity in *Pten*-deficient neurospheres. Likewise, the strong expression of Ki-67, a widely used marker for cell cycle commitment, as well as the up-regulation of various cyclins, is in line with the enhanced proliferation potential of *Pten* null neural stem/progenitor cells.

In summary, the loss of PTEN enhances G_0 cell cycle exit and self-renewal capacity and decreases growth factor dependence. These mechanisms collectively might increase the available pool of self-renewing cells that allow the accumulation of further mutational events (44). PTEN loss may also promote tumor progression by providing tumor initiating cells a self-renewal mechanism. Further study of PTEN′s function in human brain cancer stem cells, especially the G_0-G_1 cell cycle regulation, may provide both mechanistic insights and targets for treatment of glioblastoma multiforme.

Materials and Methods

Neurosphere Culture. Cortices were dissected from E14 embryos in ice-cold buffer (15 mM Hepes/$NaHCO_3$/25 mM glucose in Hanks' balanced salt solution-Ca^{2+} and Mg^{2+} free). After removal of the meninges, tissues were incubated in dissection buffer containing papain (Worthington) and DNase I (Worthington) for 10 min at 37°C, quenched with Ovomucoid protease inhibitor, and then dissociated with fire-polished Pasteur pipettes into single-cell suspensions. Cells were then cultured at a low density of 5 cells per μl by using an established neurosphere culturing system (45). The following supplements were added to the Neurobasal media: 1:50 B27, 1:100 Pen-Strep, 2 mM L-glutamine (all from GIBCO/BRL), 2 μg/ml heparin (Sigma), and 20 ng/ml FGF2 (PeproTech). Cells were incubated at 37°C in the presence of 5% CO_2. Additional FGF2 was added every third day, and cultures were passaged every 7–14 days, depending on the size of the spheres. During each passage, spheres were enzymatically and mechanically dissociated with 0.05% Trypsin-EDTA and fire-polished glass pipettes and then reseeded at the same density. For each animal and passage, cells were seeded in three separate dishes and the number of neurospheres is calculated as mean ± SD.

For growth factor-dependent assays, cells from MUT ($n = 3$) and WT ($n = 3$) forebrains were resuspended at 10 cells per μl in Neurobasal medium (GIBCO) supplemented with B-27 (GIBCO), 2 mM L-glutamine in 24-well dishes, and FGF2 was added daily at concentrations indicated. For determining neurosphere number and diameter, neurospheres were plated onto acid-treated, polyL-lysine (0.1 mg/ml) and laminin (25 μg/ml, Becton-Dickinson) coated glass coverslips (Carolina Biological Supply). Ten random view fields per sample were taken within 20 min after plating. A minimum cutoff of 50 μm diameter was used in defining a neurosphere as spheres below this cutoff were not reliably multipotent (unpublished observations).

Passage Efficiency. The time interval between each passage was determined by the size of the spheres. Spheres were passaged when diameters ranged between 75 and 150 μm. A culture was terminated when there were not enough cells to reseed a 10-ml culture at a density of 5 cells per μl. An entire experiment was terminated when there was not at least one MUT and one control in the group.

Sphere Counts, Diameter Measurements, and Multilineage Differentiation. After plating an aliquot of spheres onto polyL-lysine-coated coverslips, the number of spheres were counted and calculated as per 1,000 cells originally plated. The relative sphere count in Fig. 1*C* was first calculated as an average of sphere counts at each passage, then presented as the fold difference between MUT and WT ($n = 14$). MCID software (Imaging Research, St. Catherines, ON, Canada) was used to measure neurosphere diameters.

To test the capacity for multilineage differentiation of neural stem/progenitor cells, spheres were centrifuged, and media containing FGF2 was replaced with differentiation media: Neurobasal, 1:50 B27, 1:50 L-glutamic acid, 0.5 mM L-glutamine, and 1:100 pen-strep. Aliquots of ≈20–100 spheres were plated on polyL-lysine-coated (Sigma) coverslips (Fisher) in 24-well plates and allowed to differentiate for 5–6 days before staining for neurons (Tuj1, Berkeley Antibody; or MAP2, Chemicon), astrocytes (GFAP, DAKO), and oligodendroctyes (O4, Chemicon). Hoechst and propidium iodide were both used for nuclear counter staining.

Cell Cycle Analysis. Dissection of E14.5 forebrains was performed as described above. After dissociation, cells were either directly subjected to flow cytometric analysis or plated in Neurobasal medium (GIBCO) supplemented with B-27 (GIBCO) at 10 cells per μl for 7 days. FGF2 was added daily at 10 ng/ml. Neurospheres were then dissociated in buffer containing papain (Worthington) and DNaseI (Worthington) and subjected to cell cycle analysis.

Freshly dissociated brain or neurospheres were stained for DNA and RNA content by using 7-amino-actinomycin D (7AAD) and pyronin Y, respectively. Cells were suspended in 0.5 ml of a nucleic acid staining solution staining buffer [0.15 M NaCl in 0.1 M phosphate citrate buffer (Sigma), containing 5 mM EDTA (Sigma), 0.5% BSA (fraction V, Sigma), and 0.02% saponin (Sigma)]. Five microliters of 1 mg/ml 7AAD (Sigma) was then added to each tube to a final concentration of 10 μg/ml. The cells were incubated at room temperature in 7AAD solution for 20 min, then cooled on ice for at least 5 min before washing

the cells with 1 ml of cold PBS, and then resuspended in 0.5 ml of cold NASS buffer containing 10 μg/ml actinomycin D (Sigma). Cells were cooled on ice for 10 min before the addition of 5 μl of 0.1 mg/ml pyronin Y (PolyScience, Wilmington, Pa.), and left on ice for a minimum of 10 additional min before acquisition of flow cytometric data. This protocol was adapted from Schmid *et al.* (22). All flow cytometry was done on a Becton-Dickinson FACScalibur flow cytometer and analyzed by using FLOWJO analysis software (Treestar).

Control experiments were performed in parallel, in which the cell cycle inhibitory drug *N*-butyrate was added to the neurosphere cultures. The position of the vertical axis in the DNA/RNA plots in Fig. 3 marks the division between the G_1A and G_1B stages of the cell cycle and is determined by the *N*-butyrate-treated cells, which are blocked at the G_1A to G_1B transition. The horizontal axis marks the division between the G_1B and S phases of the cell cycle and marks the division between cells that have 2N DNA content (G_0, G_1A, and G_1B) and cells with greater than 2N DNA content (S, G_2, and M).

Microarray. Three independent replicate MUT embryos and paired control littermates were cultured as neurospheres for 14 days. Cultures were pelleted and RNA was extracted by using TRIzol reagent, and checked for quality with an Agilent 2100 Bioanalyzer. RNA from all samples was labeled with both cy3 and cy5 by using the Agilent low RNA input fluorescent linear amplification kit as per the manufacturer's instructions, and labeling was confirmed with a Nanodrop Spectrophotometer. Each paired knockout and wild-type replicate was hybridized onto two Agilent Mouse Development Oligo arrays with dye-flip for a total of six arrays. Feature extraction was performed with Agilent feature extractor software by using default settings with Lowess normalization and a standard error model to assign probability of differential regulation. To generate a gene list (Fig. 4), we selected those genes with $P < 0.001$ in five of six arrays. To generate a larger list for clustering and DAVID/EASE analysis, we used $P < 0.01$ in five of six arrays. Initial data manipulation and analyses were performed in Microsoft EXCEL. Clustering was performed with GENESPRING 6.0. Gene Ontology analysis was performed by using DAVID and EASE software available from the National Institute of Health (http://apps1.niaid.nih.gov/david). For Fig. 4, we used the DAVID set to level 5.

We thank Dr. Paul Mischel and members of our laboratories for helpful comments and suggestions. M.G. was partially supported by the Swiss National Science Foundation. J.D.D. was supported by a Howard Hughes Medical Institute Predoctoral Fellowship. D.D.S.-A. was supported by an Amgen/Esther Hayes AIDS Institute Graduate Fellowship. This work was supported by grants from Henry Singleton Brain Research Program (to H.W. and H.I.K.) and The James S. MacDonnell Foundation (to H.W.); by National Institutes of Health Grant NS38439 and The Brain Tumor Society (to X.L.); and by National Institute of Mental Health Grant 65756 and the Jonsson Comprehensive Cancer Center (to H.I.K.).

1. Li, J., Yen, C., Liaw, D., Podsypanina, K., Bose, S., Wang, S. I., Puc, J., Miliaresis, C., Rodgers, L., McCombie, R., *et al.* (1997) *Science* **275,** 1943–1947.
2. Steck, P. A., Pershouse, M. A., Jasser, S. A., Yung, W. K., Lin, H., Ligon, A. H., Langford, L. A., Baumgard, M. L., Hattier, T., Davis, T., *et al.* (1997) *Nat. Genet.* **15,** 356–362.
3. Li, J., Simpson, L., Takahashi, M., Miliaresis, C., Myers, M. P., Tonks, N. & Parsons, R. (1998) *Cancer Res.* **58,** 5667–5672.
4. Liaw, D., Marsh, D. J., Li, J., Dahia, P. L., Wang, S. I., Zheng, Z., Bose, S., Call, K. M., Tsou, H. C., Peacocke, M., *et al.* (1997) *Nat. Genet.* **16,** 64–67.
5. Nelen, M. R., van Staveren, W. C., Peeters, E. A., Hassel, M. B., Gorlin, R. J., Hamm, H., Lindboe, C. F., Fryns, J. P., Sijmons, R. H., Woods, D. G., *et al.* (1997) *Hum. Mol. Genet.* **6,** 1383–1387.
6. Myers, M. P., Stolarov, J. P., Eng, C., Li, J., Wang, S. I., Wigler, M. H., Parsons, R. & Tonks, N. K. (1997) *Proc. Natl. Acad. Sci. USA* **94,** 9052–9057.
7. Maehama, T. & Dixon, J. E. (1998) *J. Biol. Chem.* **273,** 13375–13378.
8. Myers, M. P., Pass, I., Batty, I. H., Van der Kaay, J., Stolarov, J. P., Hemmings, B. A., Wigler, M. H., Downes, C. P. & Tonks, N. K. (1998) *Proc. Natl. Acad. Sci. USA* **95,** 13513–13518.
9. Stambolic, V., Suzuki, A., de la Pompa, J. L., Brothers, G. M., Mirtsos, C., Sasaki, T., Ruland, J., Penninger, J. M., Siderovski, D. P. & Mak, T. W. (1998) *Cell* **95,** 29–39.
10. Lee, J. O., Yang, H., Georgescu, M. M., Di Cristofano, A., Maehama, T., Shi, Y., Dixon, J. E., Pandolfi, P. & Pavletich, N. P. (1999) *Cell* **99,** 323–334.
11. Sun, H., Lesche, R., Li, D.-M., Liliental, J., Zhang, H., Gao, J., Gavrilova, N., Mueller, B., Liu, X. & Wu, H. (1999) *Proc. Natl. Acad. Sci. USA* **96,** 6199–6204.
12. Stiles, B., Groszer, M., Wang, S., Jiao, J. & Wu, H. (2004) *Dev. Biol.* **273,** 175–184.
13. Groszer, M., Erickson, R., Scripture-Adams, D. D., Lesche, R., Trumpp, A., Zack, J. A., Kornblum, H. I., Liu, X. & Wu, H. (2001) *Science* **294,** 2186–2189.
14. Fraser, M. M., Zhu, X., Kwon, C. H., Uhlmann, E. J., Gutmann, D. H. & Baker, S. J. (2004) *Cancer Res.* **64,** 7773–7779.
15. Backman, S. A., Stambolic, V., Suzuki, A., Haight, J., Elia, A., Pretorius, J., Tsao, M. S., Shannon, P., Bolon, B., Ivy, G. O. & Mak, T. W. (2001) *Nat. Genet.* **29,** 396–403.
16. Kwon, C. H., Zhu, X., Zhang, J., Knoop, L. L., Tharp, R., Smeyne, R. J., Eberhart, C. G., Burger, P. C. & Baker, S. J. (2001) *Nat. Genet.* **29,** 404–411.
17. Marino, S., Krimpenfort, P., Leung, C., van der Korput, H. A., Trapman, J., Camenisch, I., Berns, A. & Brandner, S. (2002) *Development (Cambridge, U.K.)* **129,** 3513–3522.
18. Yue, Q., Groszer, M., Gil, J. S., Berk, A. J., Messing, A., Wu, H. & Liu, X. (2005) *Development (Cambridge, U.K.)* **132,** 3281–3291.
19. Gage, F. H. (2000) *Science* **287,** 1433–1438.
20. Seaberg, R. M., Smukler, S. R. & van der Kooy, D. (2005) *Dev. Biol.* **278,** 71–85.
21. Hanahan, D. & Weinberg, R. A. (2000) *Cell* **100,** 57–70.
22. Schmid, I., Cole, S. W., Korin, Y. D., Zack, J. A. & Giorgi, J. V. (2000) *Cytometry* **39,** 108–116.
23. Alam, S., Sen, A., Behie, L. A. & Kallos, M. S. (2004) *Biotechnol. Bioeng.* **88,** 332–347.
24. Miron, M., Verdu, J., Lachance, P. E., Birnbaum, M. J., Lasko, P. F. & Sonenberg, N. (2001) *Nat. Cell Biol.* **3,** 596–601.
25. Eisen, M. B., Spellman, P. T., Brown, P. O. & Botstein, D. (1998) *Proc. Natl. Acad. Sci. USA* **95,** 14863–14868.
26. Geschwind, D. H., Ou, J., Easterday, M. C., Dougherty, J. D., Jackson, R. L., Chen, Z., Antoine, H., Terskikh, A., Weissman, I. L., Nelson, S. F. & Kornblum, H. I. (2001) *Neuron* **29,** 325–339.
27. Hemmati, H. D., Nakano, I., Lazareff, J. A., Masterman-Smith, M., Geschwind, D. H., Bronner-Fraser, M. & Kornblum, H. I. (2003) *Proc. Natl. Acad. Sci. USA* **100,** 15178–15183.
28. Galli, R., Binda, E., Orfanelli, U., Cipelletti, B., Gritti, A., De Vitis, S., Fiocco, R., Foroni, C., Dimeco, F. & Vescovi, A. (2004) *Cancer Res.* **64,** 7011–7021.
29. Singh, S. K., Clarke, I. D., Hide, T. & Dirks, P. B. (2004) *Oncogene* **23,** 7267–7273.
30. Hill, C., Hunter, S. B. & Brat, D. J. (2003) *Adv. Anat. Pathol.* **10,** 212–217.
31. Mischel, P. S. & Cloughesy, T. F. (2003) *Brain Pathol.* **13,** 52–61.
32. Brat, D. J., Castellano-Sanchez, A., Kaur, B. & Van Meir, E. G. (2002) *Adv. Anat. Pathol.* **9,** 24–36.
33. Tropepe, V., Sibilia, M., Ciruna, B. G., Rossant, J., Wagner, E. F. & van der Kooy, D. (1999) *Dev. Biol.* **208,** 166–188.
34. Sinor, A. D. & Lillien, L. (2004) *J. Neurosci.* **24,** 8531–8541.
35. Molofsky, A. V., Pardal, R., Iwashita, T., Park, I. K., Clarke, M. F. & Morrison, S. J. (2003) *Nature* **425,** 962–967.
36. Kippin, T. E., Martens, D. J. & van der Kooy, D. (2005) *Genes Dev.* **19,** 756–767.
37. Morshead, C. M., Reynolds, B. A., Craig, C. G., McBurney, M. W., Staines, W. A., Morassutti, D., Weiss, S. & van der Kooy, D. (1994) *Neuron* **13,** 1071–1082.
38. Jorgensen, P., Nishikawa, J. L., Breitkreutz, B. J. & Tyers, M. (2002) *Science* **297,** 395–400.
39. Fabrizio, P., Pozza, F., Pletcher, S. D., Gendron, C. M. & Longo, V. D. (2001) *Science* **292,** 288–290.
40. Stocker, H. & Hafen, E. (2000) *Curr. Opin. Genet. Dev.* **10,** 529–535.
41. Schneider, B. L., Zhang, J., Markwardt, J., Tokiwa, G., Volpe, T., Honey, S. & Futcher, B. (2004) *Mol. Cell. Biol.* **24,** 10802–10813.
42. Dolznig, H., Grebien, F., Sauer, T., Beug, H. & Mullner, E. W. (2004) *Nat. Cell Biol.* **6,** 899–905.
43. Nakano, I., Paucar, A. A., Bajpai, R., Dougherty, J. D., Zewail, A., Kelly, T. K., Kim, K. J., Ou, J., Groszer, M., Imura, T., *et al.* (2005) *J. Cell Biol.* **170,** 413–427.
44. Reya, T., Morrison, S. J., Clarke, M. F. & Weissman, I. L. (2001) *Nature* **414,** 105–111.
45. Reynolds, B. A. & Weiss, S. (1992) *Science* **255,** 1707–1710.